Arabian Journal of Geosciences (2020) 13: 119
https://doi.org/10.1007/s12517-020-5096-3

ORIGINAL PAPER

# Detailed characterization of micronano pore structure of tight sandstone reservoir space in three dimensional space: a case study of the Gao 3 and Gao 4 members of Gaotaizi reservoir in the Qijia area of the Songliao basin

Yilin Li[1,2] · Yunfeng Zhang[1,2] · Hang Fu[1,2] · Qiang Yan[1,2]

Received: 4 July 2018 / Accepted: 8 January 2020 / Published online: 24 January 2020


**Abstract**

Tight sandstone samples from the Gao 3 and Gao 4 members of Gaotaizi reservoir in Qijia area of the northern Songliao Basin were targeted as the main research objects in this paper. Through micro/nano CT technology and auto skeleton module and connectivity module in avizo software, three-dimensional models for the micro pore structure of Gaotaizi tight sandstone in the research area were constructed. The experimental results demonstrate that types of reservoir space include intergranular dissolution pores, intragranular dissolution pores, and micro-fractures, indicating remarkable microscopic heterogeneity with characteristics of a continuous distribution in a micronano scale. Under the micro scale, different physical property and sedimentary microfacies of tight reservoir show various pore structure characteristics in three-dimensional space, with the primary front of pore throats mainly distributed in 0.6~1.5 μm. Under the nanoscale, micro heterogeneity is remarkable, with the primary front of pore throats distributed in 40~100 nm. In addition, the nanopore distribution pattern in three-dimensional space mainly includes the nanopores in the granules and the nanofractures, of which the latter type plays a crucial role in connecting nanopores and migration of nano oil and gas migration; at the same time, this paper verify the digital core experimental results by using MICP technology. With the further development of big data technology and deep learning technology, three-dimensional digital core technology based on micro/nano CT technology will become an important technology applied in the exploration and development of unconventional oil and gas.

**Keywords** Qijia area · Tight sandstone · Micropore structure · Digital core technology

## Introduction

Tight oil is an important resource in the field of unconventional oil and gas in recent years, extolled as “black gold” by the petroleum industry community (Jia et al. 2012). Tight oil exploration and development has accomplished a significant progress, represented by Bakken tight oil in the North America Williston Basin (Zhang et al. 2013).Tight oil has been mainly distributed in Qingshankou formation of Songliao basin, China (Shi et al. 2015, Li et al. 2016), Yanchang formation of Ordos basin, China (Zhang et al. 2015), Lucaogou formation in Junggar basin, China (Wu et al. 2016), etc. The central depression in the northern Songliao basin has a resource potential of over $10 \times 10^8$ t of tight sandstone oil, which is an important replacement resource for Daqing oilfield (Wang et al. 2016). In recent years, domestic and foreign scholars have studied the distribution law (Shi et al. 2015), accumulation pattern (Yuan et al. 2016), and accumulation stage of tight oil in Gaotaizi oil

Responsible Editor: Abdullah M. Al-Amri

✉ Yilin Li
liyilindaqing@163.com

✉ Yunfeng Zhang
94073505@qq.com

Hang Fu
2711057181@qq.com

Qiang Yan
412234179@qq.com

[1] Department of Earth Sciences, Northeast Petroleum University, Daqing 163318, Heilongjiang, China

[2] Oil and Gas Reservoir Forming Mechanism and Resource Evaluation Key Laboratory, Daqing 163318, Heilongjiang, China

layer (Si et al. 2018), three-dimensional pore structure in a single sample of tight reservoir single was characterized by three dimensional digital core technology in the Qijia area Li et al. 2016; Zhang et al. 2016), detailed and contrastive analysis of micronano pore structure of different samples in Qijia area is relatively weak.

Three-dimensional digital core technology is a core analytical measurement method arising in the unconventional field in recent years; it has been applied in pore structure analysis of tight sandstone (Bai et al. 2013a, 2013b) and natural gas hydrate (Dong et al. 2018), and digital petrophysical analysis of coal (Fang et al. 2018),which can three-dimensionally digitize the distribution of pores and throats, and has been widely used in the characterization of microscopic pore structure for tight reservoirs in recent years. The micro/nano CT scanning experiment for characteristics of microscopic samples from the tight sandstone reservoir of Triassic Yanchang Formation in Ordos Basin was conducted, which quantitatively evaluated the pore throat size, shape, and connectivity of tight sandstone samples in the micronano scale respectively (Bai et al. 2013a, 2013b). Dong et al. (2018) quantitatively characterized the pore throat radius and microscopic connectivity of gas hydrate reservoirs, Fang et al. (2018) described the digital petrophysical characteristics of coal and rock based on three-dimensional digital core technology by MATLAB, Avizo software, and comsol software, which have quantitatively characterized the pore-throat size, shape and connectivity, and providing a new way for the digital core analytical method. At present, there are mainly three mainstream ways of the three-dimensional digital core model. The first one is the construction of three-dimensional digital core based on micro/nano CT scanning experiment (Bai et al. 2013a, 2013b; Liu et al. 2014; Dewanckele et al. 2012; Prodanović et al. 2006; Wang et al. 2016; Zhang 2017). The second one is the establishment of digital cores through the three-dimensional modeling method of the focused ion beam scanning electron microscope (FIB-SEM) (Keller et al. 2013; Ambrose et al. 2010; Curtis et al. 2012). The third one is the construction of three-dimensional digital core based on two-dimensional image (such as casting thin section and scanning electron microscope) (Zhang et al. 2010; Hazlett 1997; Yao et al. 2013; Yang et al. 2016). It deserves to be declared that among the above three methods, this paper focuses on building three-dimensional digital core based on micro/nano CT scanning experiment. Compared with the experimental analysis technologies such as mercury injection and scanning electron microscope, the three-dimensional digital core technology can qualitatively analyze and quantitatively evaluate the pore throat size, connectivity, and shape, having the advantages of non-destructive and fast scanning imaging for the rock samples in a full range, as well as a visual observation of microscopic pore distribution, tight oil speciation, and so on.

Tight reservoirs have different scales in space, including the application of sediment-diagenetic facies in reservoir scale (Wang et al. 2019) and the application of micro analysis and testing methods in micronano scale research (Jiang et al. 2014). The effective integration of integrate macro- and microscale parameters is a hot research topic. Taking samples from Gaotaizi tight sandstone reservoir of Qingshankou Formation in Qijia area, Songliao basin, as the research objects, in this paper, the pore size of tight sandstone reservoir in the study area can be divided into two categories, mainly includes micropores (500~0.5 μm) and nanopores (< 500 nm). This paper has achieved the visual extraction of the pore throat network model at different microscales and the quantitative characterization of pore throat parameters, through the method of micro/nano CT technology combined with autoskeleton module and connectivity module in avizo software; compared with the previous research (Zhang et al. 2016), the three dimensional models were optimized, which can characterize the pore distribution and the connectivity rate of pores accurately. The research indicates that the micro/nano CT technology has a broader prospect in the future unconventional oil exploration and development, which lays a foundation for the multiscale study of tight reservoir.

## Regional geological conditions

The research area mainly includes the south of Qijia area, Qiping area, and Longhubao area; the study area is about 2000 km$^2$ (Fig. 1). The study area is located near the oil generation center of Qijia sag with adequate source of oil mainly distributed in the Gao 3 and Gao 4 members of Gaotaizi oil reservoir in Qingshankou Formation, which belongs to the deposit of large river delta plain and delta front (Li et al. 2016). Sedimentary facies type includes sheet sand of outer delta-front facies, estuary dam of inner delta-front facies, distributary channel, and shallow lake sand bars (Shi et al. 2015). The formation of Gao 3 and Gao 4 members of Gaotaizi oil reservoir is a tight contact type between source rock and reservoir, which is main source of tight oil in Daqing oilfield.

## The basic characteristics of tight sandstone reservoir

### Petrologic feature

Rocks of Gao 3 and Gao 4 reservoirs in the research area are mostly lithic feldspathic sandstone and feldspar

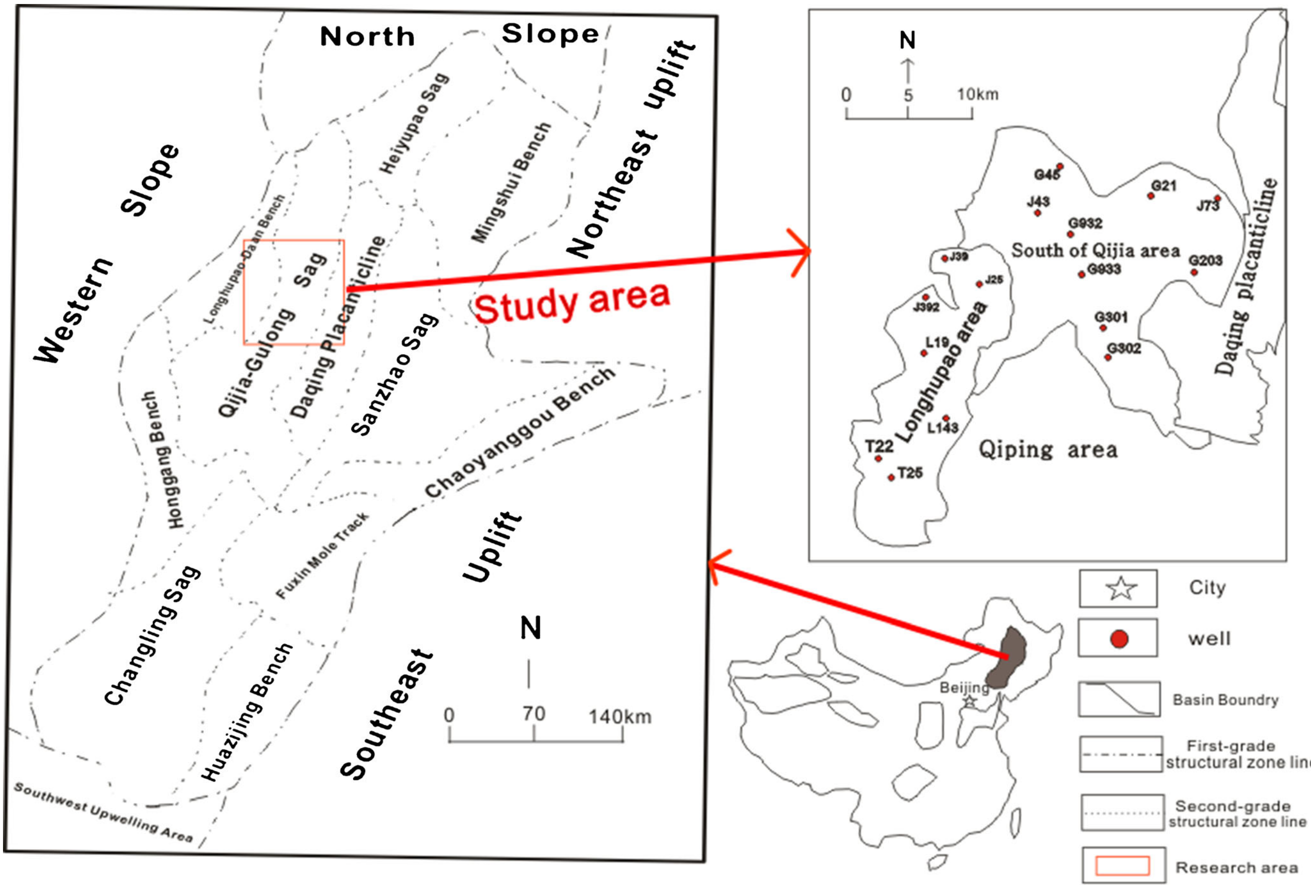


**Fig. 1** Location of the study area (Hang 2018, Li et al. 2016)

lithic sandstone; the contents of quartz, feldspar, and detritus are basically equal (Fig. 2), feldspar is mainly sodium feldspar, accounting for 33.27% (Fig. 3). Lithology is mainly siltstone and argillaceous siltstone (Shi et al. 2015, Li et al. 2016). The cement is mainly calcite (Fig. 3). Clay minerals is mainly illite and chlorite, illite accounts for 2.71%, chlorite accounts for 1.28%, and pyrite accounted for about 1.03%, which is the associated mineral of tight oil (Fig. 3).

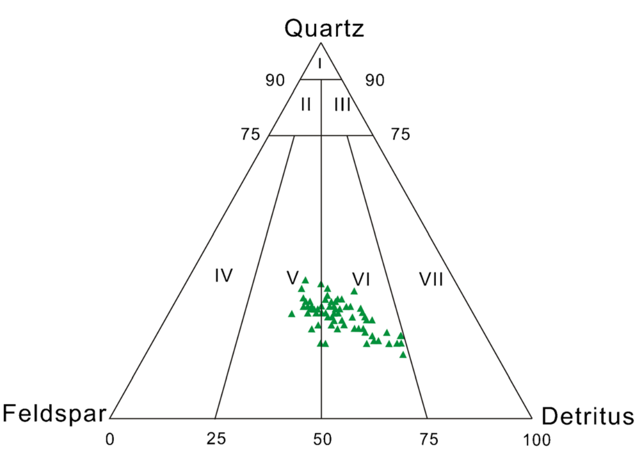


**Fig. 2** Rock composition triangle of the study area

## Macroscopic characteristics of porosity and permeability

A total of 191 samples are used to conduct statistical analysis for the porosity and horizontal permeability in Gao 3 and Gao 4 members of Gaotaizi reservoir. Statistical results showed that the average porosity of Gao 3 and Gao 4 is 8.08%. Horizontal permeability is generally $0.01 \times 10^{-3}$~$1 \times 10^{-3}$ μm$^2$, with about 50% samples less than $0.05 \times 10^{-3}$ μm$^2$. Drawing the crossplot of porosity and permeability of the study area, the figure illustrates that there is a correlation between porosity and permeability (Fig. 4). According to the reservoir quality classification standard SY/T 6285-2011 of the oil and gas industry in China, reservoirs in Qijia area are mainly tight reservoir, with relatively poor physical property (Li. et al. 2016). The average porosity and permeability of Gao 3 reservoir are better than that of Gao 4 reservoir on the plane. Areas with high value of porosity and permeability are mostly concentrated in the northwest, while the south is mainly tight reservoirs.

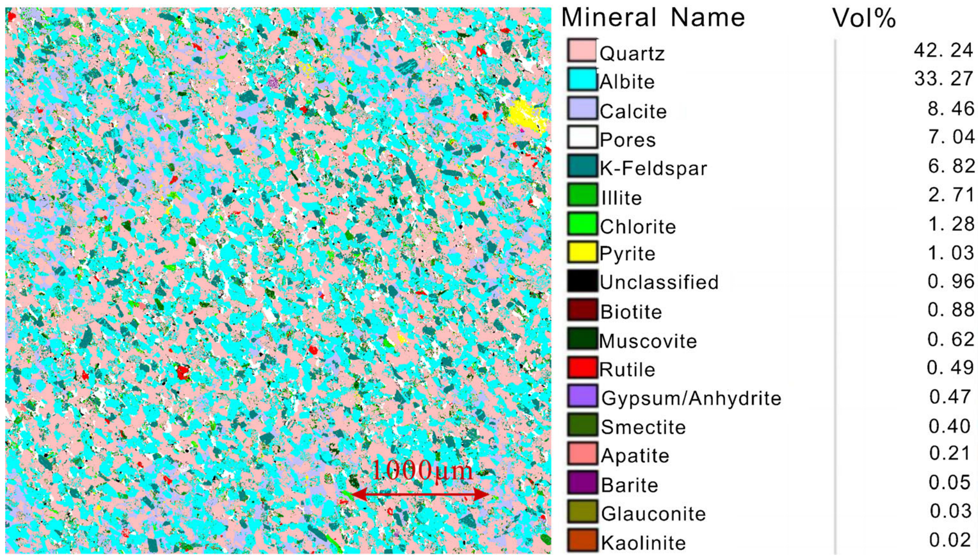


**Fig. 3** QEMSCAN analysis results of Well G933 (Li et al. 2016)

## Reservoir space feature with microscopic scales

### Pore structure characteristics with 2D scales

Unconventional testing methods such as FIB-SEM analysis technology are utilized combined with the casting thin sections; these methods were applied to the analysis of 2D pore structure characteristics. The result shows that intergranular dissolution pores (Fig. 5a), intragranular dissolution pores (Fig. 5b), and microscopic fractures (Fig. 5c) constitute the main microscopic space of Gaotaizi oil reservoir in Qijia area under 2D Scales; two-dimensional pore characteristics analysis cannot effectively study pore morphology and quantitative characteristics of pores under different scales; it is necessary to use three-dimensional digital core technology for further analysis.

### Pore structure characteristics with 3D scales

In this paper, Phoenix Nanotom S CT scanner (resolution 0.5~12 μm) and Ultra- XRM-L200 nano CT scanner (resolution 16 nm or 65 nm) were used to carry out the experiment; two-dimensional gray images of different microscopic scales were achieved by CT scanning (Fig. 6); this research focuses on three-dimensional model for the pore throat structure of Gaotaizi tight reservoir in Qijia area at different scales through the built-in mathematical model of avizo software based on two-dimensional gray images by micro/nano CT technology. The experimental result shows that the overall microscopic connectivity of Gaotaizi tight reservoir is relatively weak, and the microscopic space can be divided into two scales: the micro scale and the nano scale, both with remarkable microscopic heterogeneity. Microscopic reservoir space, microscopic pore throat distribution, and connectivity corresponding to different scales are variant (Fig. 7, Fig. 8, and Table 1). Overall, Gaotaizi tight reservoir in Qijia area has the best connectivity under the microscale, which is the main research direction of microscopic pore structure in the future.

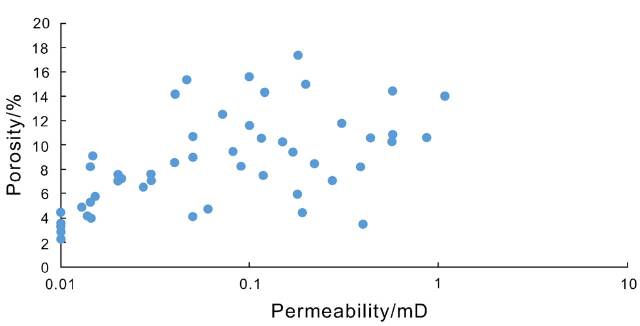


**Fig. 4** The crossplot of porosity and permeability of the study area

#### Microscaled pore structure characteristics

Under the micro scale, different physical property and sedimentary microfacies of tight reservoir show various pore structure characteristics in three-dimensional space (Fig. 7). The primary front of the pore is distributed in 0.6~1.5 μm with serious "trailing" phenomenon (Fig. 7c, f, and i, Table 1). The distribution of the pore throat mainly includes sheet shape and isolated shape. Through the contrast of different samples in different microfacies and physical properties, it shows that subaqueous distributary channel microfacies with relative high porosity and connectivity rate in the three-dimensional reservoir space is characterized by sheet shape (Fig. 7a, b), 35.7% occupation of the main distribution range of pores (0.8~1.5 μm) among the

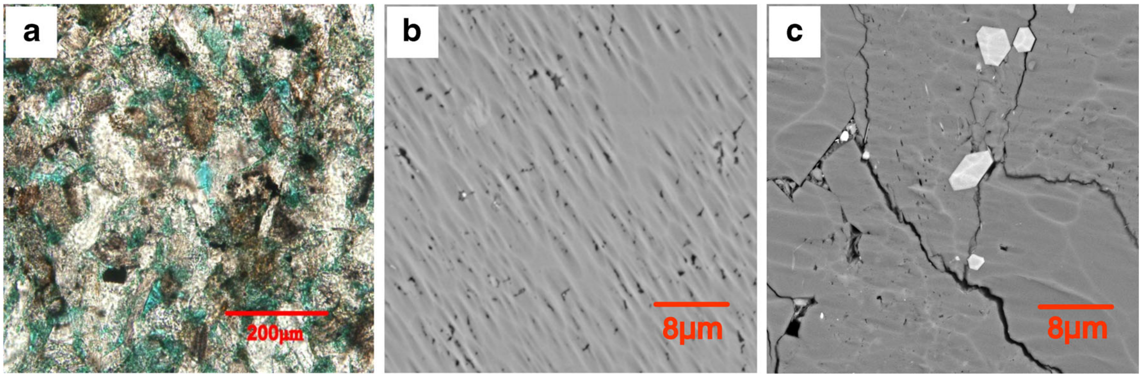


**Fig. 5** Pore types of tight sandstone reservoir space in Qijia area **a** intergranular dissolution pores, siltstone, Well G933 at 2212.48 m by casting thin section with polarized light × 20; **b** intragranular dissolution pores, siltstone, Well G933 at 2205.06 m by FIB-SEM; **c** stereotype micro-fractures, argillaceous siltstone, Well G933 at 2205.06 m by FIB-SEM

overall distribution of pore and about 90.5% occupation of the connected pore (Table 1). Estuary bar microfacies with low physical property in the three-dimensional reservoir space is characterized by coexist of sheet shape and isolated shape (Fig. 7d, e), relatively concentrated pore radius, 59.4% occupation of the main distribution range of pores among the overall distribution of the pore and the connectivity of pores is poor (Table 1). Sheet sand microfacies with relative low porosity and permeability is characterized by isolated shape in three-dimensional space (Fig. 7g, h), highly concentrated distribution of pore radius, 70.4% occupation of the main distribution range of pores (0.8~1.2 μm) area among the overall distribution of the pore, and the connectivity of pores is poor (Table 1). Generally as for pore radius, pore connectivity, pore volume, and pore surface area, these microscopic pore structure parameters of the distributary channel microfacies are superior to that of the estuary bar microfacies and sheet sand microfacies, which are better beneficial to the micronano oil and gas accumulation. Samples of the sheet

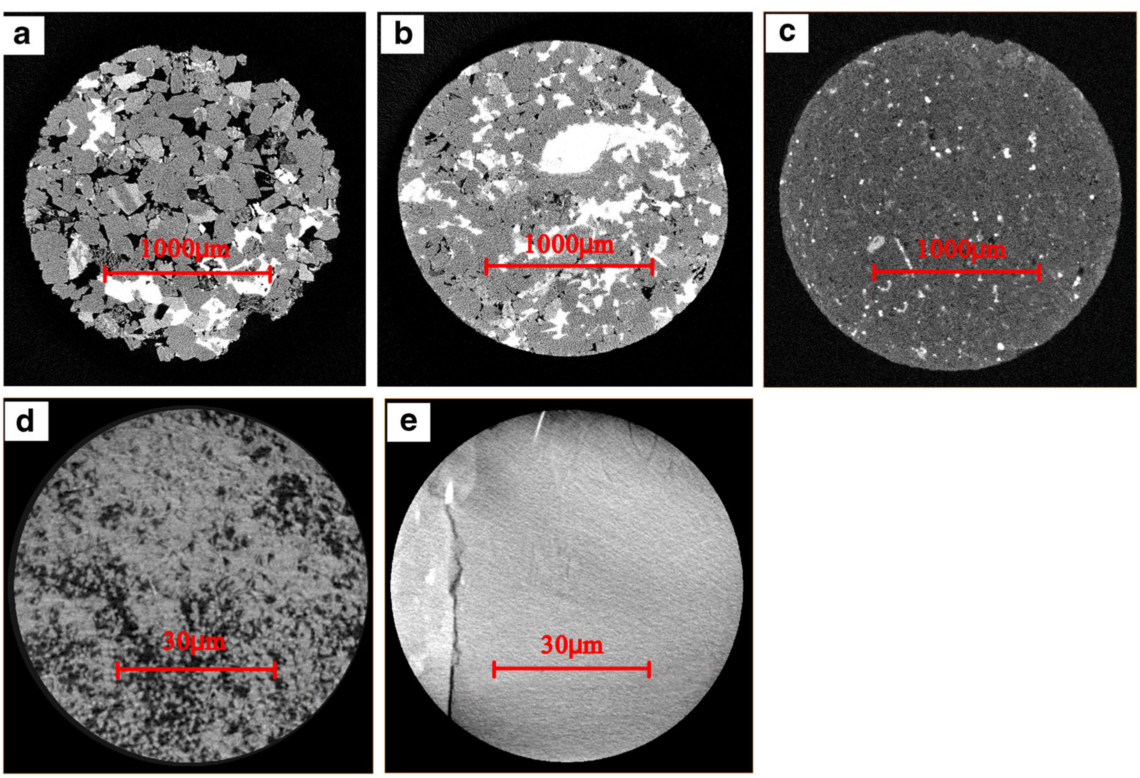


**Fig. 6.** Two-dimensional grayscale images based on micro/nano CT (deep black area represents pores) **a** Well Jin393 at 1981.23 m, micro CT, resolution: 1 μm; **b** Wel G933 at 2111.8 m, micro CT, resolution 1 μm; **c** Well L291 at 1910.53 m, micro CT, resolution:1 μm; **d** Well G933 at 2205.36 m, nano CT, resolution: 65 nm; **e** Well G933 at 2201.01 m, nano CT, resolution 65 nm.

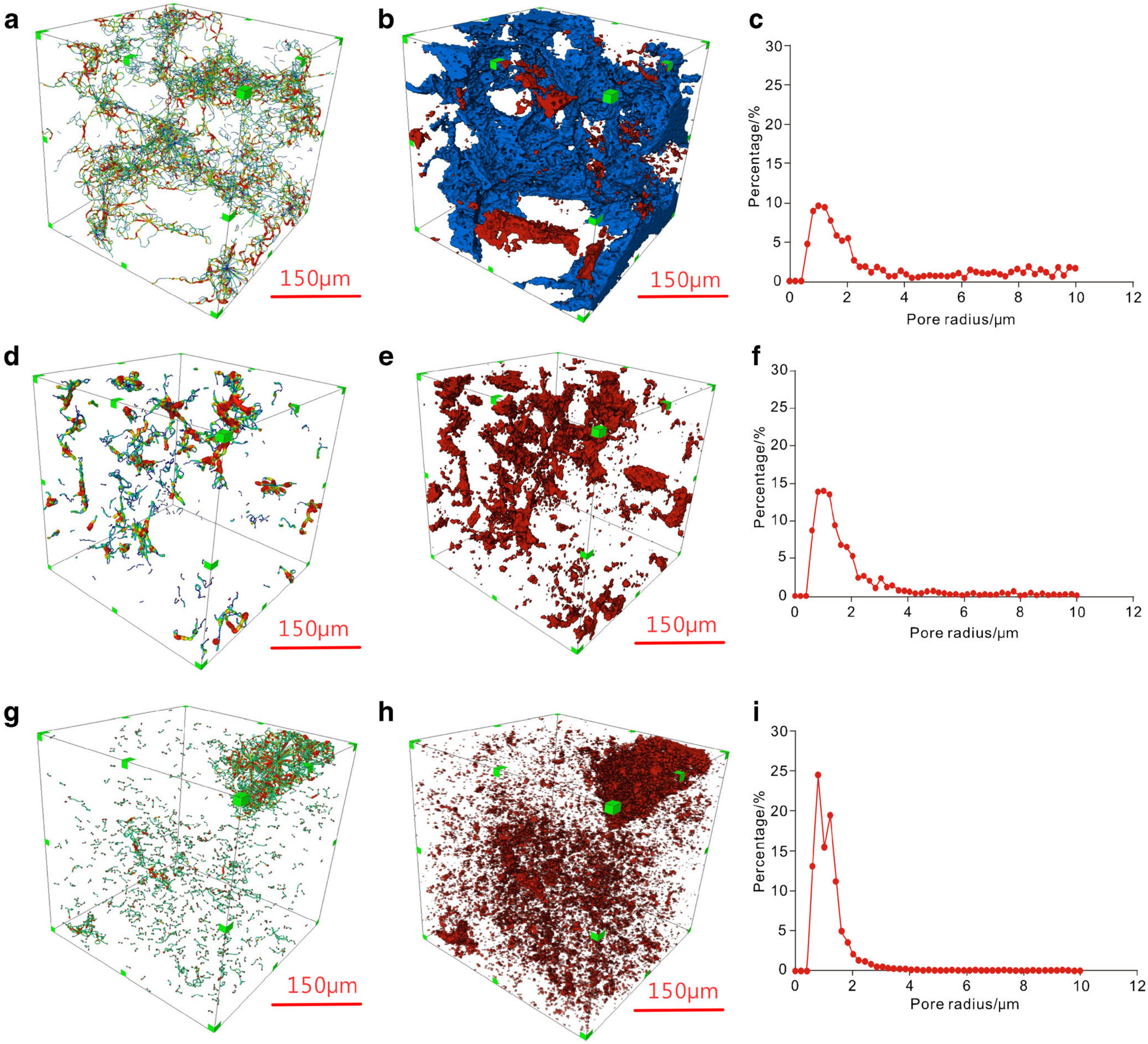


**Fig. 7** Digital core model and pore parameters histogram of Gaotaizi tight reservoir space in Qijia area under the micro scale. **a** Pore network model based on auto skeleton module, well Jin393 at 1981.23 m; **b** Connectivity mode based on connectivity module (blue pores represent for the interconnected pores; red pores represent for the isolated pores), Well Jin393 at 1981.23 m; **c** Pore radius distribution, Well Jin393 at 1981.23 m; **d** Pore network model based on auto skeleton module, Well G933 at 2111.8 m; **e** Connectivity mode (blue pores represent for the interconnected pores; red pores represent for the isolated pores), Well G933 at 2111.8 m; **f** Pore radius distribution, Well G933 at 2111.8 m; **g** Pore network model based on auto skeleton module, Well L291 at 1910.53 m; **h** Connectivity mode based on connectivity module (blue pores represent for the interconnected pores, red pores represent for the isolated pores), Well L291 at 1910.53 m; **i** Pore radius distribution, Well L291 at 1910.53 m

sand microfacies have an absolute advantage in the quantity of the pore.

## Nanoscaled pore structure characteristics

Under the nanoscale, pore primary front is distributed in 40~100 nm. The nanopore distribution pattern in three-dimensional space mainly includes two kinds (Zhang et al. 2016): nanointragranular pores (Fig. 8a, b) and nanofractures according to the experimental results from auto skeleton module and connectivity module in avizo software (Fig. 8d, e) (compared with the previous research, the three-dimensional models were optimized; this method can characterize the connectivity rate of nanopores accurately). Nanointragranular pores are characterized by isolated small pellet in three-dimensional space pattern with relatively uniform distribution (Fig. 8a, b); 53.8% occupation of the main distribution range of pores among the overall distribution of the pore and the

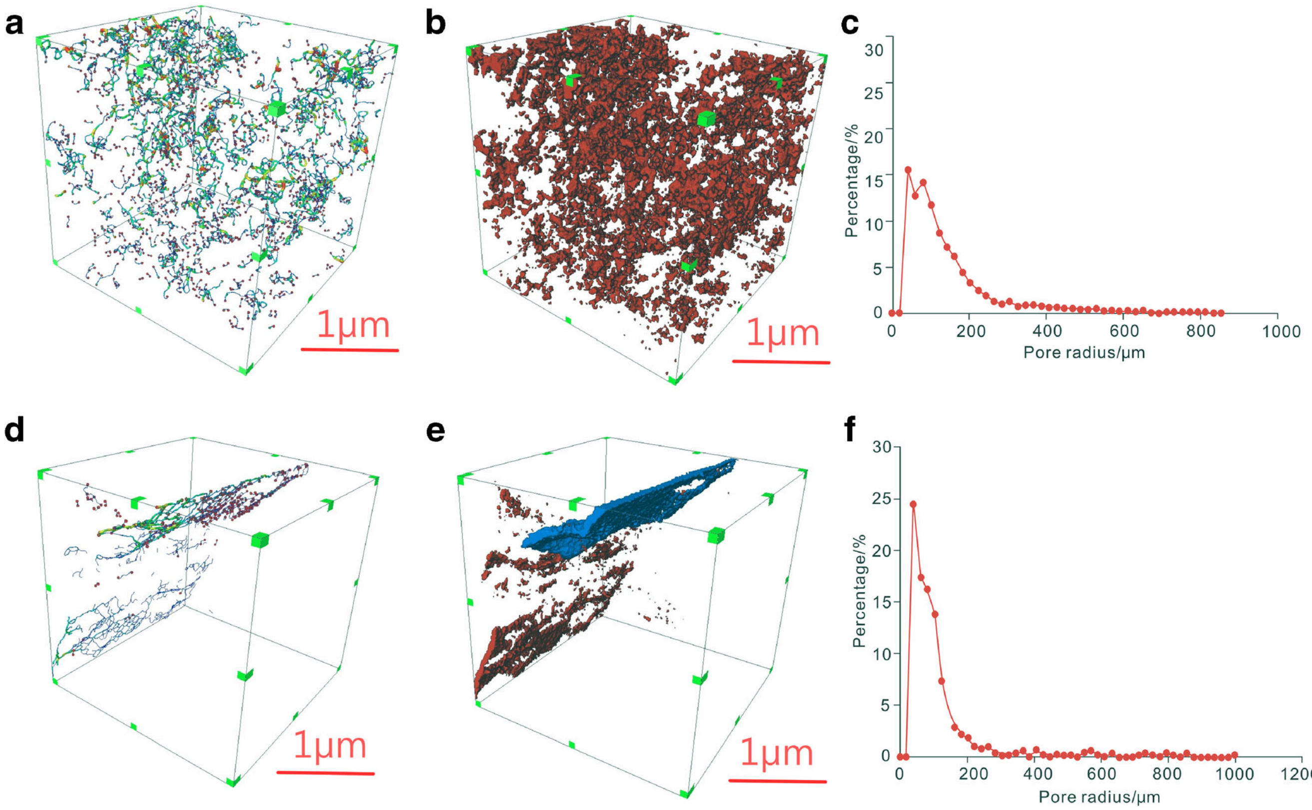


**Fig. 8** Tight sandstone digital core model and pore radius distribution of Gaotaizi tight reservoir space in Qijia area under the nano scale. **a** Nanopore type in pore network mode based on auto skeleton module, Well G933 at 2205.36 m; **b** Nanopore type in connectivity mode (blue pores represent for the interconnected pores, red pores represent for the isolated pores), Well G933 at 2205.36 m; **c** Nanopore type in pore radius distribution, Well G933 at 2205.36 m; **d** Nanofracture type in nanofracture network model, Well G933 at 2201.01 m; **e** Nanofracture type in connectivity model (blue pores represent for the interconnected pores; red pores represent for the isolated pores), Well G933 at 2201.01 m; **f** Nanofracture type in pore radius distribution, Well G933 at 2201.01 m

connectivity of pores are poor (Fig. 8c and Table 2). Nanofractures have the characteristics of banded pores as the main pore in three-dimensional space, relatively concentrated distribution (Fig.8c,8d), 71.6% occupation of the main distribution range of pores among the overall distribution of pore and about 50.9% occupation of the connected pore (Fig. 8f

**Table 1** Quantitative analysis of core samples with different porosity and permeability under the micro scale

| Well ID | Jin393 | G933 | L291 |
|---|---|---|---|
| Sample depth/m | 1981.23 m | 2111.8 m | 1910.53 |
| Digital core porosity/% | 11.12 | 3.56 | 1.58 |
| Effective porosity of digital core/% | 10.6 | 0 | 0 |
| Isolated porosity of digital core/% | 0.47 | 3.56 | 1.58 |
| Percentage of connected pores% | 90.5 | 0 | 0 |
| Main distribution range of pore radius/μm | 0.8~1.5 | 0.6~1.4 | 0.8~1.2 |
| Total pore volume/$\mu m^3$ | 3,020,656 | 570,985 | 426,714 |
| Maximum pore volume/$\mu m^3$ | 30,243 | 33,278 | 29,657 |
| Average pore surface area/$\mu m^2$ | 954.56 | 234.48 | 33.87 |
| Number of pores and throats | 3829 | 1469 | 13,052 |
| The three-dimensional distribution pattern of pore throat | Sheet | Sheet, isolated | Isolated |
| Corresponding sedimentary microfacies | Subaqueous distributary channel microfacies | Estuary bar microfacies | Sheet sand microfacies |

**Table 2** Quantitative analysis of microscopic characteristics under the nanoscale

| Distribution type of the microscopic reservoir space | Nanopore type | Nanofracture type |
|---|---|---|
| Well ID | G933 | G933 |
| Effective porosity of digital core/% | 0 | 0.56 |
| Isolated porosity of digital core/% | 2 | 0.54 |
| Connectivity rate of pores/% | 0 | 50.9 |
| Primary front of pore radius/nm | 40~100 | 40~100 |
| Average throat radius/nm | 110 | 213 |
| Maximum pore volume /nm$^3$ | $3.88 \times 10^9$ | $7.28 \times 10^9$ |
| Total pore volume/nm$^3$ | $1.97 \times 10^{11}$ | $7.17 \times 10^{10}$ |
| Number of pores and throats | 4287 | 603 |

and Table 2). On the whole, nanopore type is superior to nanofracture type in pore quantity and pore volume, nanopore type is good reservoir space of nano oil and gas, while nanofracture type is superior to nanopore type in connectivity rate of pores, throat radius, and pore distribution pattern (Table 2), playing a crucial role in connecting nanopores and migration of nano oil and gas migration.

## Discussion

This research focuses on three-dimensional digital core through the built-in mathematical model of avizo software; in this study, avizo software was applied to analyze and process functions in this study; avizo software cannot only build the three-dimensional micropore structure of tight reservoirs, at the same time, tight reservoir microscopic connectivity was described; however, the data source digital core technology is reliable? This section focuses on MICP technology to validate reliability of digital core data.

MICP technology is one of the major approaches to the study of the microscopic pore structure; MICP can quantitatively evaluate the pore structure; at the same time, MICP technology can quantitatively evaluate the seepage of the reservoir capacity; MICP technology solve many problems of exploration and development of oil field. This section focuses on MICP technology to authenticate digital core experiment results analysis; only the micron scale digital core analysis of experimental results were verified due to experiment precision; the experimental results are as follows (Table 3, Fig. 9); experimental comparison results show that the pore radius distribution differences between MICP experiment results, and the digital core experiment results are small, but there are some errors; the reasons of the errors are as follows: (1) due to the different scales of the two methods, digital core experiment samples is relatively small (the experimental samples are about 2 mm in diameter, MICP experiment samples are about 2.5 cm in diameter), different experiment scale will cause some errors. (2) Binarization segmentation process (distinguish between porosity and rock matrix) in digital core experiment may produce some errors; therefore, digital core models need MICP experiment analysis results for reference, providing reliable boundary condition for the rock physical simulation. Digital core technology can obtain three-dimensional pore structure characteristics of different scales, with the improvement of resolution, the sample volume decreases; the representative of digital core models is smaller. MICP technology, NMR technology, and other numerical analysis technologies can measure pore volume and pore diameter distribution, but these methods cannot

**Table 3** The statistical table of MICP parameters (partial)

| Well ID | H | *K* | *φ* | *Sp* | *Skp* | Mp | SH(%) | | *We* | Pcd (MPa) |
|---|---|---|---|---|---|---|---|---|---|---|
| | (m) | ($10^{-3}$ μm$^2$) | (%) | | | | *Smax* (%) | *Sr* (%) | (%) | |
| | | | | | | (μm) | | | | |
| Jin393 | 1981.2 m | 0.185 | 12.24 | 3.247 | 0.396 | 2.5 | 86.160 | 57.821 | 32.892 | 0.192 |
| G933 | 2111.8 m | 0.065 | 7.52 | 2.832 | 0.213 | 1.0 | 86.343 | 55.406 | 35.831 | 0.192 |
| L291 | 1910.53 | 0.032 | 4.63 | 2.016 | 0.197 | 0.4 | 95.078 | 67.488 | 29.019 | 0.468 |

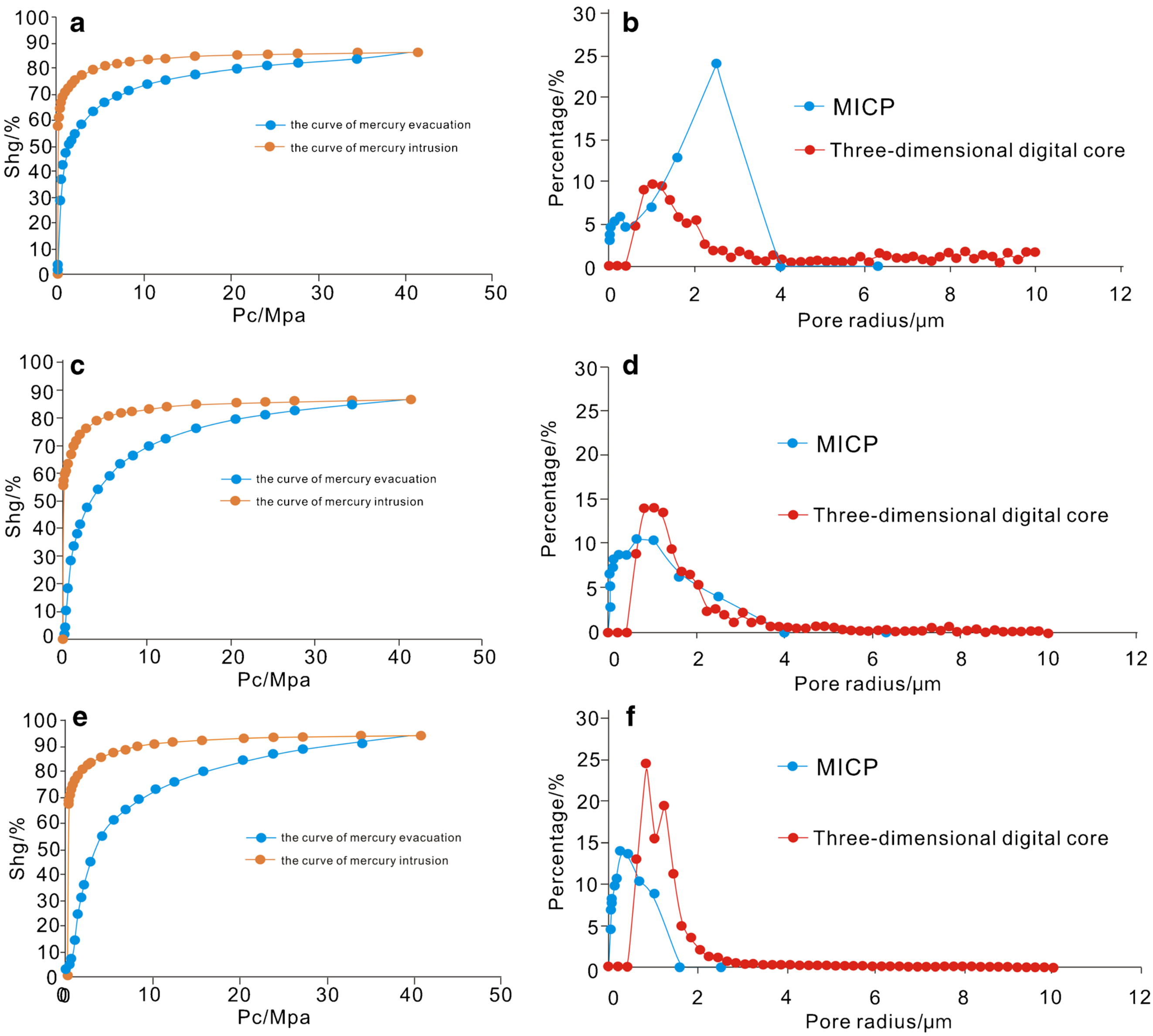


**Fig. 9** Comparison diagram between MICP result and three-dimensional digital core result of the study area. **a** Capillary pressure curve, Well Jin393 at 1981.23 m; **b** pore radius distribution according to MICP and three-dimensional digital core, Well Jin393 at 1981.23 m; **c** capillary pressure curve, Well G933 at 2111.8 m; **d** pore radius distribution according to MICP and three-dimensional digital core, Well G933 at 2111.8 m; **e** capillary pressure curve, Well G933 at 2111.8 m; **f** connectivity mode, Well L291 at 1910.53 m; **g** pore network model, Well L291 at 1910.53 m; **h** Pore radius distribution according to MICP and three-dimensional digital core, Well L291 at 1910.53 m

obtain visualization analysis of three-dimensional pore structure characteristics; multi-scale microscopic fusion technology is currently the study hotspot of microscopic pore structure of tight sandstone.

H-Sample depth; K-Permeability; φ-Porosity; Sp-sorting coefficient; Skp-skewness; Kp-kurtosis; Mp-Main peak of pore radius; SH-Mercury saturation; Smax-Maximum intake of mercury; Sr-Final surplus; We-Maximum mercury removal efficiency of the instrument; Pcd-displacement pressure

## Conclusions

By the micro/nano CT technology, the paper builds a three-dimensional model for the micronano pore structure of the Gaotaizi tight reservoir in Qijia area. Under the microscale, different physical property and sedimentary microfacies of tight reservoir show various pore structure characteristics in three-dimensional space. And under the nanoscale, nanopore distribution pattern mainly includes nanopores and nanofractures, indicating a remarkable heterogeneity. The nanofracture type plays an important role in connecting nanopores. This paper verify the digital core experimental results by using MICP technology; the results show that the pore radius distribution differences between MICP technology three-dimensional digital core technology are small, but there are some errors. With the further development of big data technology and deep learning technology, three-dimensional digital core technology based on micro/nano CT will become an important technical mean to participate in the exploration and development of tight reservoirs.

**Funding information** This work was financially supported by Science Foundation for Young Scientists of Northeast Petroleum University (Grant No. 2018QNL-46); National Natural Science Foundation of China (Grant No.41772144)

## References

Ambrose RJ, Harman RC, Diaz-Campos M et al (2010) New pore-scale considerations for shale gas-in-place calculations. C , Society of Petroleum Engineers Unconventional Gas Conference, Pittsburgh, Pennsylvania, SPE Paper, 131772

Bai B, Zhu R, Wu S et al (2013a) Multi-scale method of nano(micro)-CT study on modifications inside natural building stones by means of high resolution X-ray CT. Pet Explor Dev 40:329–333

Bai Y, Zhao J, Zhao Z et al (2013b) Tight oil reservoir-forming conditions and reservoir characteristics in Zhidan area in Ordos basin. Oil & Gas Geology 34:631–639

Curtis ME, Sondergeld CH, Ambrose RJ et al (2012) Microstuctural investigation of gas shales in two and three dimensions using nanometer-scale resolution imaging. AAPG Bull 96:665–667

Dewanckele J, De Kock T, Boone MA et al (2012) 4D imaging and quantification of pore structure modifications inside natural building stones by means of high resolution X-ray CT. Sci Total Environ 416: 436–448

Dong H, Sun J, Lin Z et al (2018) Quantitative characterization and characteristics analysis of microscopic pore structure in natural gas hydrate based on CT scanning. Journal of China Univ Pet (Ed Nat Sci) 42:40–49

Fang, Huihuang ., Sang, Shuxun. , Liu, Shiqi,, et al.2018, Study of digital petrophysical analysis method based on micro-focus X-ray tomography: a case study from no. 3 coal seam of Bofang mining area in southern Qinshui basin, Coal Geol Explor, 46,167–181

Hang F (2018) The tight reservoir microscopic classification of southern part of Qijia area in Songliao Basin. IOP Conference Series: Earth Environ Sci 113:01–04

Hazlett RD (1997) Statistical characterization and stochastic modeling of pore networks in relation to fluid flow. Math Geol 29:801–822

Jia Chengzao, Zou Caineng, Li Jianzhong et al (2012). Assessment criteria, main types, basic features and resource prospects of the tight oil in China. Acta Petrolei Sinica 33:343–350

Jiang Y, Chen L, Jiang C et al (2014) Characterization techniques and trends of pore structure of tight reservoirs. Geol Sci Technol Information 33:63–69

Keller LM, Schetz P, Erin R et al (2013) Characterization of multi-scale microstructural features in Oplinus Clay. Microporous Mesoporous Mater 170:83–94

Li Y-l, Yun-Feng Z, Shu-Li Y et al (2016) Characterization of the pore space in tight sandstone reservoirs from macroscopic and microscopic perspectives: a case study of Gaotaizi reservoir in Qijia area, the Songliao Basin. Oil Gas Geol 37:915–922

Liu, Xiangjun., Zhu Honglin., Liang Lixi.,2014, Digital rock physics of sandstone based on micro-CT technology, Chin J Geophys, 57, 1133–1140

Prodanović M, Lindquist WB, Seright RS (2006) Porous structure and fluid partitioning in polyethylene cores from 3D X-ray microtomographic imaging. J Colloid Interface Sci 298:282–297

Shi L, Wang Z, Zhang G et al (2015) Tight oil forming conditions and distribution regularities in Qijia Area in Songliao basin, petroleμm exploration and development. 42:44–50

Si S, Zhao J, Liu J et al (2018) Determination of accumulation periods and relative maturity of tight oil and gas in Gaotaizi oil reservoir of Qijia area by using fluorescence spectrum of oil inclusions. China Petroleum Explor 23:78–86

Wang Y, Meng Q'a, Liang J et al (2016) Tight oil exploration in northern Songliao basin. China Petroleum Explor 20:44–53

Wang YZ, Cao YC, Ma BB, Xi KL, Cheng X, Song MS (2019) Identification of sedimentary-diagenetic facies and implications for reservoir quality: evidence from the Eocene coarse-grained deposits in the Dongying Depression, Bohai Bay Basin, China. Arab J Geosci 23:489–507

Wu H, Hu W, Cao J, Wang X et al (2016) A unique lacustrine mixed dolomitic-clastic sequence for tight oil reservoir within the middle Permian Lucaogou formation of the Junggar basin, NW China: Reservoir characteristics and origin. Mar Pet Geol 76:115–132

Yang Y F., Wang C C., Yao J., et al. 2016. A new method for microscopic pore strucure analysis in shale matrix. J Eatth Sci. 41, 1067–1073

Yao J, Wang CC, Yang YF et al (2013) The construction method and microscopic flow simulation of carbonate dual pore network model (in Chinese). J Sci Sin-Phys Mech Astron 43:896–902

Yuan qing, Luo qun, li nan et al (2016) The tight oil accumulation mode in the Gaotaizi oil reservoir in south of Qijia area. Special Oil & Gas Reservoirs 23:54–57

Zhang T, Lu DT, Li DL (2010) A method of reconstruction of porous media using a two-dimensional image and multiple-point statistics. J Univ Sci Technol China 40:271–277

Zhang Ni-ni, Liu Luo-fu, Su Tian-xi et al (2013) Comparison of Chang 7 Member of Yanchang Formation in Ordos Basin with Bakken Formation in Williston Basin and Its Significance.Geoscience 27: 1120–1130

Zhang Xiaowen, Chen Shijia,Yao Yitong et al (2015). Study on Start-Up Pressure of Charging for Super-Low Permeability Reservoir, Upper Triassic Yanchang Formation, Ordos Basin.Geological Review 61: 925–934

Zhang N-n, Liu L-f, Su T-x et al (2016) Comparison of Chang 7 member of Yanchang formation in Ordos basin with Bakken formation in Williston basin and its significance. Geoscience 27:1120–1130